Article

Chemical Modification of Birch Bark (*Betula* L.) for the Improved Bioprocessing of Cadmium(II), Chromium(VI), and Manganese(II) from Aqueous Solutions

Jarosław Chwastowski *[ID] and Paweł Staroń [ID]

Department of Engineering and Chemical Technology, Cracow University of Technology, 24 Warszawska St., 31-155 Kraków, Poland; pawel.staron@pk.edu.pl
* Correspondence: jaroslaw.chwastowski@pk.edu.pl

Abstract: This study aimed to assess the sorption capacity of a natural sorbent, specifically birch bark (BB), and its modification using chemical reagents, including nitric and hydrochloric acid, sodium hydroxide, and chloride. The objective of the chemical modification was to enhance the sorption capacity of the heavy metals cadmium(II), chromium(VI), and manganese(II). The most effective modification for adsorbing cadmium and manganese from aqueous solutions was achieved by treating the sorbent with a 0.1 M sodium hydroxide solution (BBNa). Conversely, in the case of chromium, each modification adversely affected its adsorption by the sorbent. Concentrations of the solutions were analyzed using atomic absorption spectrometry at appropriate time intervals. The adsorption process was described using Langmuir, Freundlich, and Temkin isotherms. The Freundlich isotherm provided the best fit for cadmium and chromium (R^2 = 0.988 and 0.986, respectively), while the Langmuir isotherm was most suitable for manganese (R^2 = 0.996). The sorption capacity varied for each metal ion: Cd (II)—33.13 mg/g, Cr (VI)—35.98 mg/g, and Mn (II)—24 mg/g for the highest concentration tested. This study employed pseudo–first-rate order, pseudo–second-rate order model kinetics, and the Weber–Morris model to examine the adsorption kinetics. The pseudo–second-rate order kinetics demonstrated the best fit (R^2 > 0.94) for each heavy metal, which underlines the process's chemical nature.

Keywords: bioprocessing; heavy metal ions; green chemistry; natural sorbents; kinetics

1. Introduction

Environmental pollution with heavy metals is one of the most serious environmental problems. Even small amounts of toxic heavy metals in the environment are harmful to both plant and animal life and can pose a threat to the health and lives of humans. Their presence is associated with the dynamic development of various industries, including mining, fertilizer production, fuel and stainless steel production, metal surface treatment, metallurgy, and galvanization.

Heavy metals are a group of metals and metalloids characterized by an atomic density five times greater than that of water, exceeding 4000 kg/m^3, and naturally occurring in the Earth's crust [1]. They exhibit high melting and boiling points, ductility, and malleability. These elements are efficient conductors of heat and electricity. In chemical reactions, they act as electron donors, forming simple cations and indicating their reducing properties [2].

Among heavy metals, notable examples include chromium, lead, arsenic, mercury, zinc, cadmium, copper, gold, and silver. Some metals, such as zinc, copper, and manganese, are essential for proper biological functioning, but exceeding defined limits can pose risks to living organisms. Conversely, elements like cadmium, lead, and mercury have no positive impact on organisms and are extremely harmful to the environment. Following absorption by the human body, ions of these metals associate with specific biomolecules—proteins and nucleic acids—disrupting their functions. Heavy metals that cause acute poisoning

include cadmium, mercury, zinc, and arsenic, while chronic poisonings are associated with exposure to manganese, chromium, nickel, lead, and tin. Chronic poisoning may not exhibit symptoms for a long time. They can later manifest the effects of mutagenic action, leading to damage to the nervous system and the development of cancer. The toxicity of a given metal is influenced by its environmental form. Metal ions can negatively affect organs other than their compounds. The toxicity of cadmium primarily results from the presence of Cd (II) ions, which can accumulate mainly in the liver and kidneys, causing damage to the respiratory and circulatory systems and negatively impacting fetal development [3–6]. Cadmium, lead, and mercury are considered the most dangerous and toxic heavy metals [7].

Methods employed for the removal of heavy metal ions include membrane technologies, adsorption on activated carbon [8,9], chemical precipitation, ion exchange, and electrochemical treatment [10]. Membrane technologies used for water purification include reverse osmosis, ultrafiltration, nanofiltration, and microfiltration [11]. Typically, before discharging industrial wastewater into the environment, various physicochemical and biological processes are utilized to remove contaminants. Conventional purification processes for heavy metals and dyes, such as chemical precipitation and coagulation, are expensive and inefficient. A more cost-effective and efficient method for removing toxic industrial pollutants is the use of natural biosorbents, which can serve as an alternative to costly adsorption processes using activated carbons and ion exchange resins. In addition to low costs and high efficiency, the advantages of biosorbent application include the possibility of material regeneration, heavy metal recovery, and a reduction in chemical and biological sludge formation.

The term "biosorption" refers to the binding of ions and other molecules from aqueous solutions by biomass. This process occurs due to the affinity between the adsorbate and the biosorbent. To enhance sorption capabilities, physical and chemical modifications of the surface of the sorbent are carried out, albeit at an increased cost of the applied biosorbents [12]. Bioremediation is an environmentally friendly technique that utilizes natural biological processes to remove toxic pollutants through the activity of microorganisms or organic matter [3].

This work aimed to check the sorption capacity of organic sorbent-birch bark (*Betula* L.) and its chemical modification to enhance its bioremediation properties against heavy metal ions such as cadmium(II), manganese(II) and chromium(VI) present in aqueous solutions.

The modified birch bark exhibited notable selectivity and high adsorption capacities for the target metal ions. Kinetic and equilibrium studies further elucidated the adsorption mechanisms and highlighted the potential application of chemically modified birch bark as a cost-effective and eco-friendly bioprocessor for heavy metal removal from aqueous solutions. This research contributes to the advancement of sustainable technologies for environmental remediation and underscores the importance of harnessing natural resources for mitigating anthropogenic impacts on water quality.

2. Materials and Methods

2.1. Chemicals and Sorbent Preparation

The birch bark was acquired from the market in the southeast part of Poland. The material preparation involved several steps. Firstly, the material was rinsed with distilled water to remove any solid impurities. Subsequently, it was dried at 105 °C for 24 h. Finally, the dried material was ground and sieved to achieve a uniform particle size.

In the preliminary stage of the research, the adsorption process of cadmium, chromium, and manganese ions from solutions containing their respective salts at a concentration of 250 mg/L was examined. Following this, the sorbent underwent chemical modification through exposure to 0.1 M solutions of nitric acid (V), hydrochloric acid, sodium hydroxide, and sodium chloride. The adsorption process of metals from solutions with a concentration of 250 mg/L was then repeated. Based on the obtained results, suitable modifications were selected for each heavy metal to enhance the sorption capacity of the investigated

sorbent. For cadmium and manganese, the modification with a 0.1 M NaOH solution was chosen for further investigation, while for chromium, the unmodified sorbent was utilized. All of the chemicals used in the study were of analytical grade and were obtained from Sigma-Aldrich (Steinheim, Germany). The solutions of metal ions ($K_2Cr_2O_7$, $CdSO_4$, $Mn(NO_3)_2$) and sorbent modifiers (NaOH, HNO_3, HCL, and NaCl) were prepared by dissolving the appropriate weighs in distilled water.

2.2. General Methods

Surface analysis of the chosen sorbents was conducted using scanning electron microscopy (SEM, Hitachi TM-3000, Tokyo, Japan) equipped with the EDS microanalyzer (energy-dispersive X-ray spectroscopy). Elemental analysis was conducted on a Perkin Elmer CHN analyzer type 2400 (Waltham, MA, USA). Chemical group information present in the material was obtained using the FTiR-ATR method (Thermo Scientific Nicolet iS5 spectrometer with the ATR iD7 attachment, Waltham, MA, USA). The surface area was measured using Macrometrics ASAP 2010 (Norcross, GA, USA). Initially, samples were dried at 110 °C under helium conditions for 8 h and then at 100 °C in a vacuum of 0.001 Torr for 8 h. Metal content analysis was performed using inductively coupled plasma with optical emission spectrometry (ICP-OES) in a Perkin Elmer OPTIMA 7300 DV apparatus (Waltham, MA, USA).

2.3. Bioremediation Process

The heavy metal ion bioremediation through the adsorption process was conducted in a batch system. Sorbent in the amount equal to 0.5 g was placed in 6 containers, and 40 cm^3 of the respective solution with concentrations of 50 mg/L, 100 mg/L, 150 mg/L, 200 mg/L, and 250 mg/L were added. Subsequently, the containers were placed on a rotary shaker (200 rpm/min) and filtered through syringe filters (Puradisc™ 13—PP membrane, 0.45 μm) after 5, 10, 15, 30, 60, and 90 min. The filtrate was analyzed using atomic absorption spectrometry, while the sorbent, after adsorption, underwent SEM and FTIR analysis. The maximum bioremediation was labeled as q_e and was calculated using the equation:

$$q_e = \frac{(C_0 - C_e) \cdot V}{m_e \cdot 1000} \tag{1}$$

where m_e is the mass of the sample in grams and V is the volume of the metal ion solution given in cm^3, C_0 (mg/L) is the initial concentration of metal ions, and C_e (mg/L) is the concentration of metal ions in the equilibrium. Experiments were made in triplicate, and the results were averaged. The resulting error did not exceed 5% in all of the tests.

2.4. Sorption in Equilibrium

In this particular case, three main isotherm models were used: Langmuir, Freundlich, and Temkin. The equations that were used to calculate the mentioned models are presented in Table 1.

Table 1. Linearized equations of Langmuir, Freundlich, and Temkin isotherm models.

Model	Equation
Langmuir	$\frac{C_e}{q_e} = \frac{C_e}{q_{max}} + \frac{1}{b \cdot q_{max}}$ (2)
Freundlich	$\log q_e = \log K_f + \frac{1}{n} \log C_e$ (3)
Temkin	$q_e = B \ln K_t + B \ln C_e$ (4) $B = \frac{RT}{b_t}$ (5)

where,

> q_{max}—maximum sorption capacity (mg/g);
> b—Langmuir constant (dm^3/mg);
> K_f—Freundlich constant ($mg^{1-(1/n)}dm^3)^{1/n}g^{-1}$);
> n—heterogeneity coefficient;
> K_t—constant for the maximum binding energy (dm^3/g);
> B—constant of the sorption heat (J/mol);
> R—gas constant (8.314 J mol/K);
> T—temperature (K);
> b_t—Temkin isotherm constant.

2.5. Sorption Kinetics

The kinetics of metal ion adsorption from aqueous solutions onto BB and BBNa samples were assessed through batch experiments. The uptake of metal ions was monitored at intervals from initial contact until equilibrium was attained, allowing for the determination of the adsorption rate. The kinetic process describes the rate at which the adsorption of the chosen metal ions onto the sorbent varies with time. The obtained data from the kinetic experiments for the adsorption process were analyzed using the pseudo–first-rate order, pseudo–second-rate order, and Weber–Morris diffusion models. The equation used for the above-mentioned models is presented in Table 2.

Table 2. Linearized version of sorption kinetic models.

Model	Equation
Pseudo–first-rate order	$\log(q_e - q_t) = \log q_e - \frac{k_1}{2.303}t$ (6)
Pseudo–second-rate order	$\frac{t}{q_t} = \frac{1}{k_2 q_e^2} + \frac{t}{q_e}$ (7)
Weber–Morris	$q_t = K_{id}\, t^{0.5} + I$ (8)

where,

> k_1—pseudo–first-rate order kinetics constant (1/min);
> k_2—pseudo–second-rate order kinetics constant;
> K_{id}—the intra-particle diffusion rate constant (mg/g $min^{0.5}$);
> I—intercept of the line in the Weber–Morris model.

2.6. Desorption Studies

To determine whether the sorbent can be reused, five cycles of sorption/desorption were carried out. Five different eluents at a concentration of 0.1 M were used: citric acid, acetic acid, sodium chloride, potassium chloride, and water as a control. Tests were prepared in a couple of steps. Firstly, 0.5 g of BB and BBNa were added to the 250 cm^3 Erlenmeyer flasks. Then, 100 cm^3 of Cd(II), Cr(VI), and Mn(II) solutions at a concentration equal to 400 mg/L were added to the flasks accordingly. After a specified time (5 h), the samples were filtered and dried in an oven at 105 °C for 24 h. In the next step, the dried samples were treated with the chosen eluent (40 cm^3) for 1.5 h. After this period, the concentration of metal ions in the resulting solution was measured using AAS. The desorption degree was calculated using the equation provided below:

$$R_{des} = \frac{M_{sol}}{M_{sor}} \cdot 100\% \tag{9}$$

where

M_{sol}—metal content in solution after desorption (mg); M_{sor}—metal content in sorbent after desorption (mg).

3. Results and Discussion

The SEM image of the studied materials, birch bark (BB) and birch bark modified with NaOH (BBNa), before and after the sorption process is presented in Figure 1. The morphological structure of the used materials appears undefined, porous, rough, and heterogeneous. Additionally, pores are visible on the surface, indicating the organic nature of the material. EDS analysis reveals that in all of the conducted sorption experiments, metal ions (cadmium—1A', chromium—1B', and manganese 1C') are present on the surface of both BB and BBNa materials, confirming the successful progress of the bioremediation process. The signal showing Au ions originates from the gold sputtering of the sample.
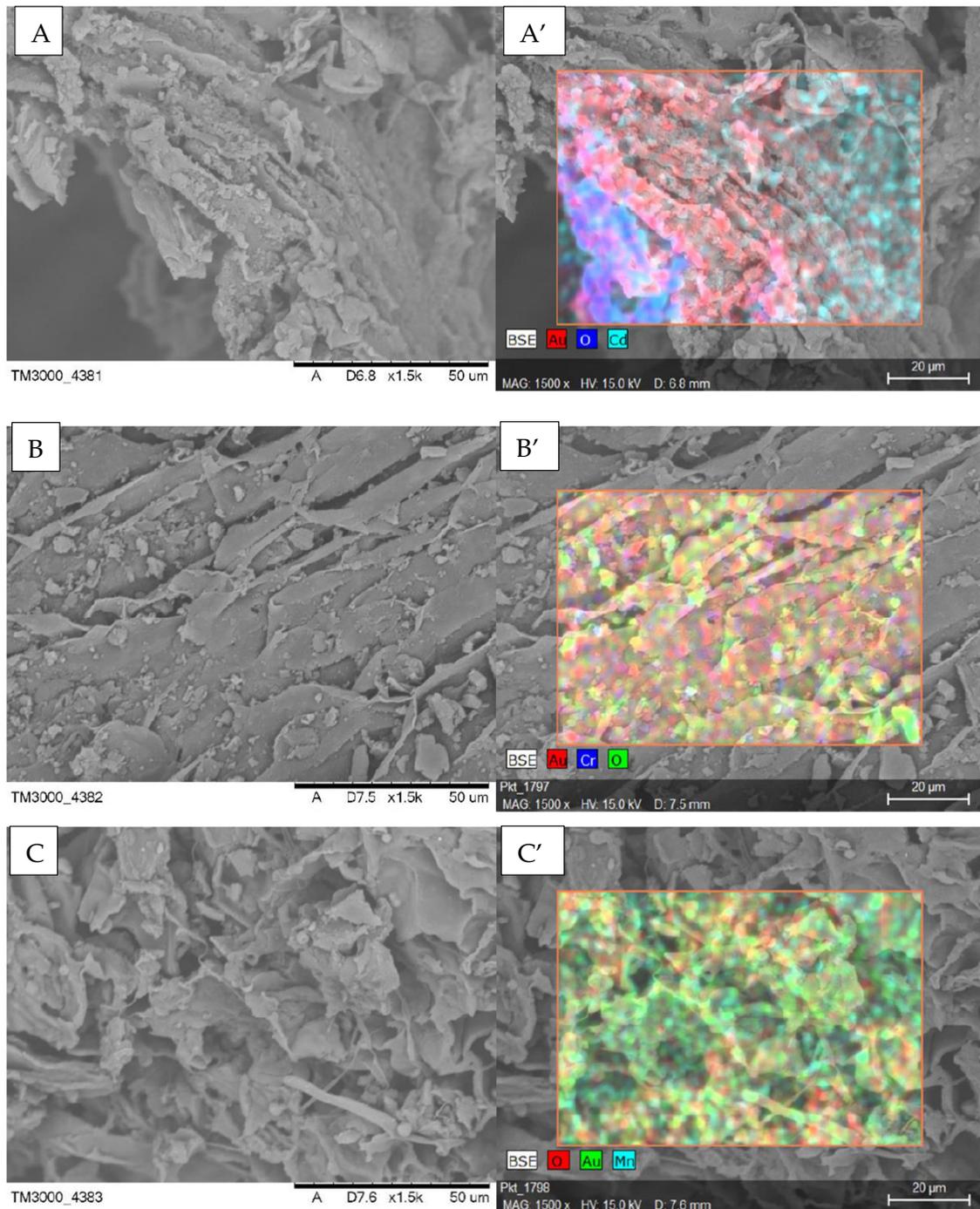
Figure 1. SEM–EDS microphotography of BB—(**B**,**B'**) and BBNa—(**A**,**A'**); (**C**,**C'**) before and after the sorption process against cadmium—A, chromium—B, and manganese—C.

Table 3 provides information on the elemental composition of adsorbents—BB and BBNa. The primary elements detected in all of the utilized sorbents are carbon and oxygen, which are typical for organic materials, consistent with the literature [4–6]. The composition of both materials is very similar, with no significant differences observed in terms of carbon (~45%) and oxygen (50%) content, which aligns with the values obtained by Song et al. (2020) [7].

Table 3. Ultimate analysis by weight (%) of BB and BBNa.

Elemental Composition (%)	Untreated Bark (BB)	Alkali-Treated Bark (BBNa)
C	44.27%	44.95%
O	50.23%	50.87%
N	0.25%	0.21%
H	4.25%	3.12%
Others	0.98%	0.85%

The specific surface area of untreated bark was measured, and the obtained value was equal to 6.12 m^2/g. For alkali-treated bark, the specific surface area was found to be 4.52 m^2/g. The possible explanation for the reduction in the surface area after the modification is pore blocking or destruction of the surface structure. The pore size distribution of used sorbents is presented in Figure 2. One can see that for untreated bark (BB), there is a high peak of the size of the pores in the range between 1.5 and 4 nm, corresponding to the mesoporous size region (Figure 2A). In the case of alkali-treated bark (BBNa), the pore size distribution shows some peaks with pore diameters of 2.2, 3.8, 4, 4.3, and 6.5 nm in the mesopore region (Figure 2B). These results show that the chemical treatment of bark results in mesopore differentiation.
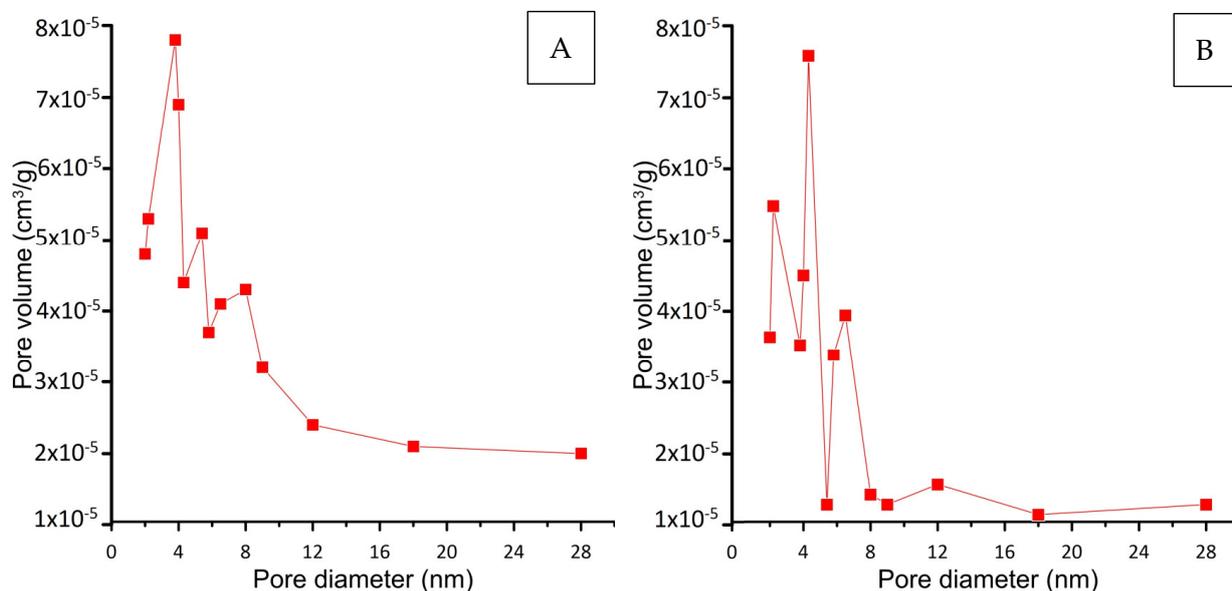
Figure 2. Pore-size distribution curves: (**A**)—untreated bark, (**B**)—alkali-treated bark.

The results found in the literature suggest that carboxyl groups are responsible for the binding of metal cations such as cadmium and manganese. It can be inferred that an increase in the number of carboxylate ligands in the biomass would enhance the binding capacity. Pectin and cellulose, which are major components of bark composition, contain methyl esters [13], which can be modified with sodium hydroxide to carboxylate ligands, further enhancing the cation-binding properties of the biomass [14]. This hypothesis is supported by the results obtained in this study, which show lower binding of chromium ions acting as anions in the water solution ($Cr_2O_7^{2-}$) using the modified sorbents.

The FTIR (Fourier transform infrared spectroscopy) analysis is provided in Figure 3 of all used sorbents and their modifications. In the wavenumber range of 3000–3700 cm^{-1}, a broad peak of maximum intensity is observed, corresponding to the stretching vibrations of C–H and hydroxyl groups –OH in cellulose [15]. For modifications with NaCl, HNO$_3$, and HCl, the signal in this range exhibits higher intensity compared to NaOH modification and unmodified bark. The signal in the range of 2900–3000 cm^{-1} is characteristic of stretching vibrations of CH$_2$ groups [16]. The peak at 1700 cm^{-1} corresponds to stretching vibrations of C=O groups, and its intensity increases for HCl, NaCl, and HNO$_3$ modifications. Peaks in the range of 1600–1500 cm^{-1} are characteristic of vibrations of the aromatic ring in lignin, and their intensity decreases for NaOH modification. The range of 1400–1300 cm^{-1} corresponds to bending vibrations of C–H bonds [17]. The peak at the wavenumber of 1000 cm^{-1} corresponds to stretching vibrations of C–O or C–O–C groups [18].
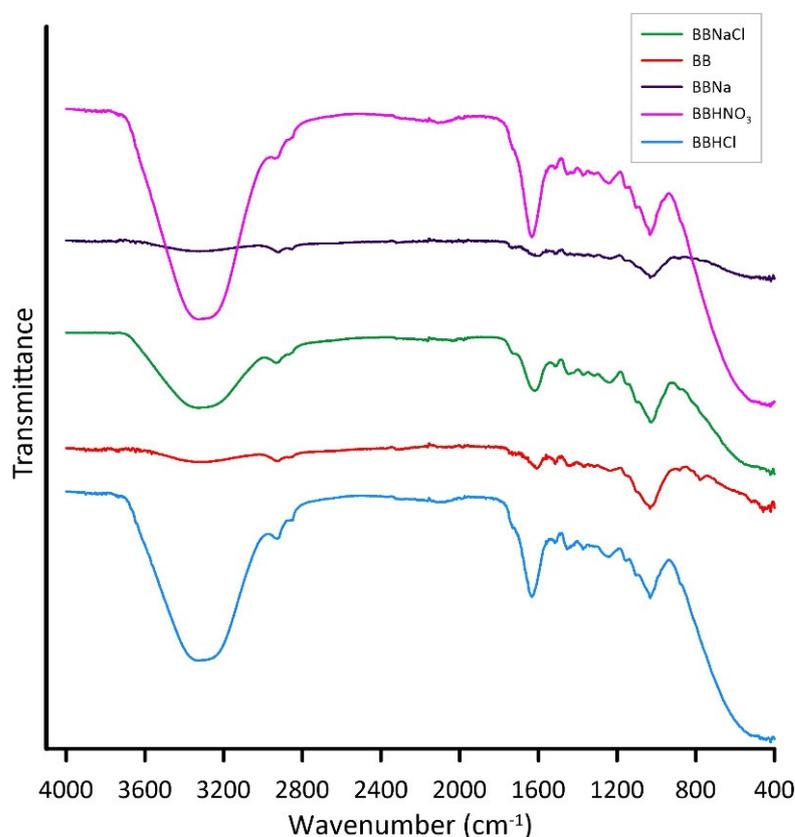
Figure 3. FTIR spectra of all materials used in the preliminary and main experiments.

To assess the sorption capacity of selected materials, equilibrium values for Cd (II), Cr (VI), and Mn (II) were calculated. Figure 4 illustrates the sorption capacity against time, depicting the highest initial metal ion concentration for each metal ion and material, along with the increasing maximum sorption capacity (q$_e$) corresponding to the rising initial concentration (C$_0$).

The results shown in Figure 4 show that the equilibrium of the bioremediation process is reached approximately 30–60 min after the start of the experiment. In the first phase of ion removal, there is a high increase in sorption capacity up to the 20th minute of the process. This phenomenon is probably connected with the increase in contact between the surface of materials and metal ions. It can be noted that the sorption capacity varies and is strictly connected to the sorbent. The highest removal capacity for cadmium and manganese is reached using modified birch bark (BBNa) and equals 33 mg/g and 13 mg/g, respectively. Chromium ions are best adsorbed by raw birch bark (BB) up to 35 mg/g.
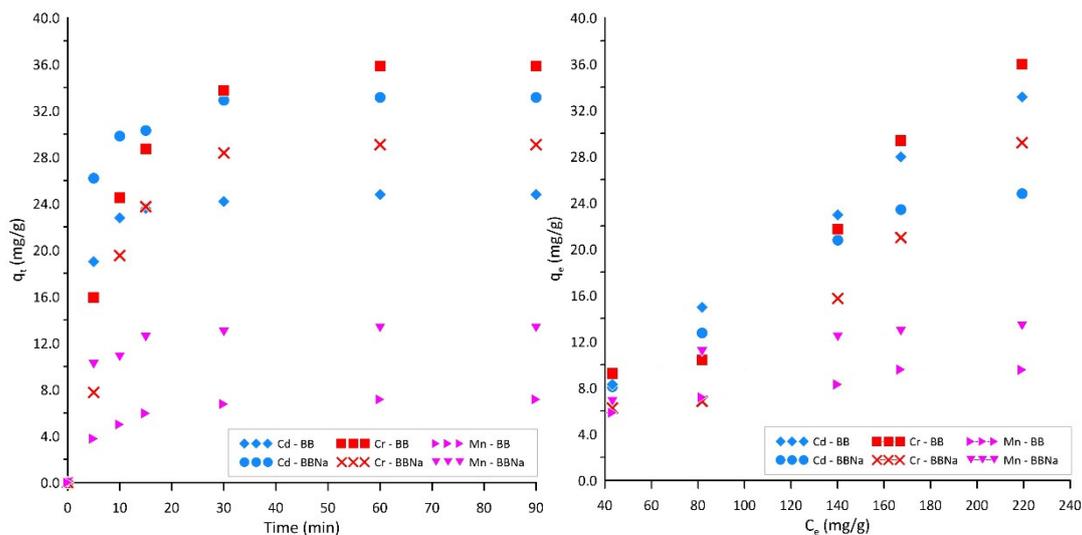
Figure 4. Sorption capacity over a specified time depends on the chosen material and sorption capacity over the initial concentration (C_0 = 250 mg/L, T = 25 °C, pH = 6).

3.1. Sorption Experiments

The bioremediation through the sorption process of manganese(II), chromium(VI), and cadmium(II) ions with the use of birch bark and its modification with sodium hydroxide solution was determined using three main isotherm models: Langmuir, Freundlich, and Temkin. In the course of experiments, it was found that the highest correlation coefficient, R^2, was fitted with the Freundlich isotherm model for chromium and cadmium ions (R^2 = 0.986 and 0.988, respectively) and the Langmuir isotherm model for manganese ions (R^2 = 0.996). The obtained results are shown in Table 4 and Figure 5. Similar results were reported for Cr(VI) ion adsorption by biosorbent derived from fertilizer industry waste [19], cadmium (II) with the use of *Cystoseria indica* brown algae [20], and coffee pulp for the removal of manganese (II) ions [21].

Table 4. Parameters of the sorption isotherm models.

Parameter	BB			BBNa		
	Cd(II)	Cr(VI)	Mn(II)	Cd(II)	Cr(VI)	Mn(II)
Freundlich						
R^2	0.944	0.986	0.449	0.988	0.973	0.897
$K_F(\text{mg}^{1-(1/n)}(\text{dm}^3)^{1/n}\text{g}^{-1})$	5.761	2.202	4.543	7.016	0.304	4.703
$1/n$	0.332	0.609	0.141	0.390	0.918	0.232
Langmuir						
R^2	0.975	0.871	0.945	0.962	0.141	0.996
K_l	0.080	0.017	0.133	0.107	0.001	0.190
Temkin						
R^2	0.904	0.874	0.394	0.943	0.880	0.898
B	4.917	11.303	1.014	6.833	12.41	0.891
K_t	1.617	0.199	55.38	1.778	0.058	3.998

3.2. Sorption Kinetics

The obtained experimental capacity values of the materials used for three different metal ions indicate that the process is time-dependent. In all three cases, the highest uptake occurs within the first 20 min of contact time and gradually increases to reach a plateau. The pseudo–first-rate order (PFO), pseudo–second-rate order (PSO), and Weber–Morris intraparticle diffusion (W–M) models were employed to fit the data obtained from the experiments. The calculated values obtained from the linearized version of the equations are presented in Table 5 and Figure 6. According to the results, the PSO model has the

highest coefficient of determination ($R^2 > 0.940$) in all tested metal and sorbent variations. This suggests that the adsorption process of all used metals and adsorbents is controlled by chemisorption (the rate-limiting step of the process). Comparing the experimental maximum sorption capacity and the one obtained from the model calculations, one can see that they are similar. It can be suggested that the chosen models describe the process well. Similar results have been reported in numerous experiments regarding kinetics [22–27]. Upon studying the results obtained using the W–M intraparticle diffusion model, it is observed that the calculated R^2 for this model is low for all metal ions and adsorbents. This implies that the bioremediation process through adsorption is not solely reliant on intra-particle diffusion but rather that more than one step affects the adsorption [28].
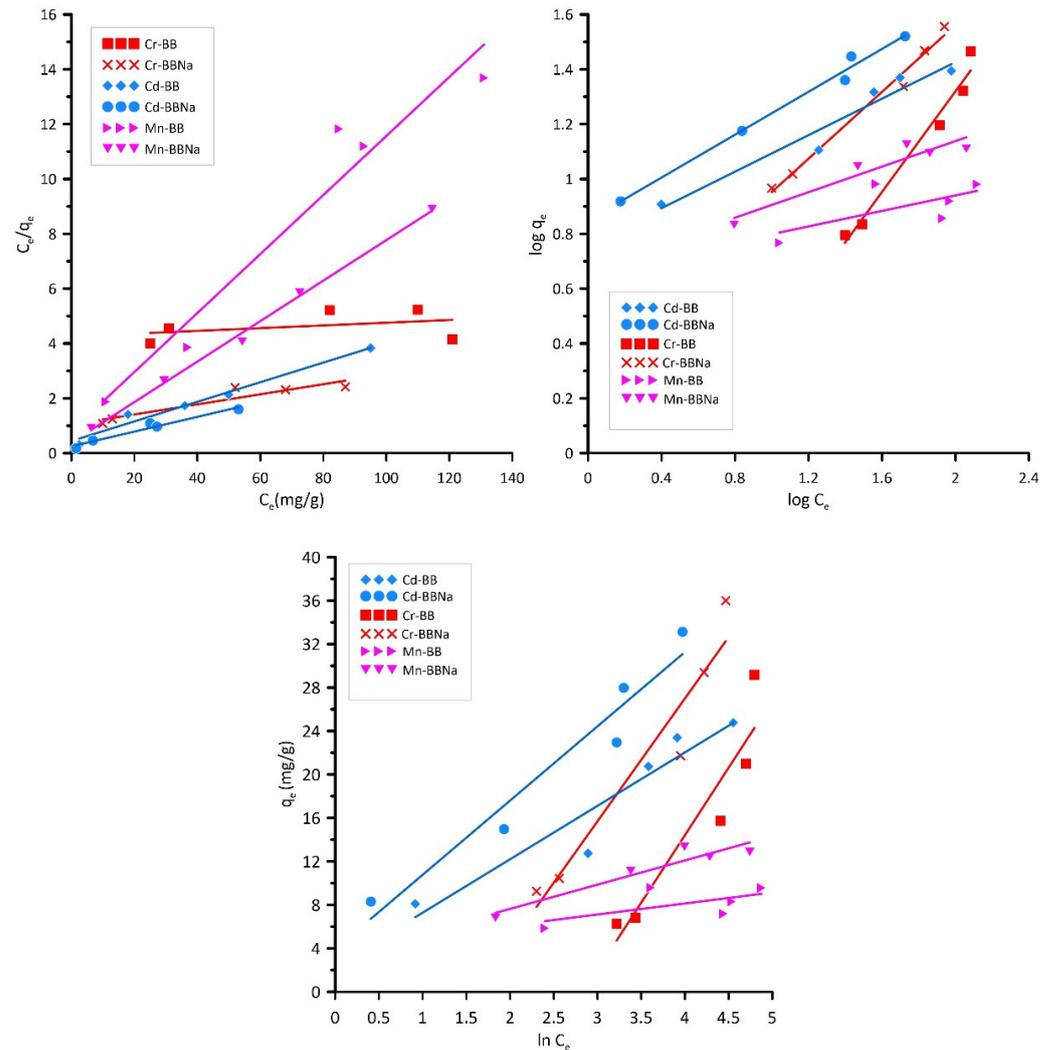
Figure 5. Linearized Langmuir, Freundlich, and Temkin Isotherm models for the Cr(VI), Cd(II), and Mn(II) bioremediation through the adsorption process with the use of BB and BBNa, respectively.

According to the kinetics and material characteristics, it can be concluded that all of the metal ions used in the study covered the surface of adsorbents and entered their pores by capillary forces. This result is strongly proven by means of SEM–EDS analysis (Figure 1). The material modification (BBNa) has better surface charge properties for the adsorption of cations (Mn, Cd). Chromium ions are supposed to also act as cations, but in water, they act as anions, which is related to the electronic configuration of chromium in its hexavalent state, thus better sorbing on unmodified birch bark (BB). Chromium(VI) has a +6 oxidation state, meaning it has lost six electrons. The electronic configuration of a neutral chromium atom is [Ar] $3d^5 4s^1$. In the hexavalent state, chromium loses its 4s electrons

and five of its 3d electrons, leaving it with an electron configuration of [Ar] $3d^0$. With an empty 3d subshell and a partially filled 4s subshell, chromium (VI) ions are more stable when they gain electrons rather than lose them. This is because gaining electrons allows them to achieve a filled or more stable electron configuration. In the case of dichromate ($Cr_2O_7^{2-}$) ions, these species have gained additional electrons to achieve a more stable state, resulting in a net negative charge. In aqueous solutions, chromate and dichromate ions readily associate with water molecules and exist as anions, contributing to the overall negative charge of the solution.

Table 5. Kinetic parameters for the adsorption of Cd(II), Cr(VI), and Mn(II) onto BB and BBNa.

Parameter	BB					BBNa				
	Cd(II) Concentration (mg/dm^3)									
	50	100	150	200	250	50	100	150	200	250
I order										
q_e	5.576	6.064	16.157	8.585	15.081	1.374	2.977	11.563	8.432	11.913
k1	0.1616	0.0627	0.0936	0.0321	0.1155	0.1178	0.0234	0.0535	0.0221	0.0540
R^2	0.9902	0.9271	0.9807	0.6088	0.8893	0.7976	0.2598	0.9632	0.7004	0.7580
II order										
q_e	8.364	13.386	20.931	23.793	25.981	8.390	13.642	22.603	27.215	34.545
k2	0.0643	0.0177	0.0070	0.0086	0.0107	0.2013	0.0996	0.0127	0.0127	0.0094
R^2	0.9997	0.9988	0.9960	0.9926	0.9970	0.9999	0.9995	0.9995	0.9967	0.9992
Weber Morris										
I	5.6520	6.5702	6.3941	11.0630	12.5089	7.1955	11.3329	11.8796	17.5199	19.8388
K_{id}	0.3628	0.8318	1.7571	1.5088	1.7814	0.1701	0.3299	1.3604	1.1495	1.8580
R^2	0.7333	0.8816	0.8391	0.8281	0.6399	0.5640	0.3486	0.8355	0.9139	0.7860
	Cr(VI) Concentration (mg/dm^3)									
	50	100	150	200	250	50	100	150	200	250
I order										
q_e	1.611	1.704	5.180	5.334	6.445	1.310	1.897	4.744	5.439	6.589
k1	0.0652	0.0261	0.0833	0.0603	0.0646	0.0451	0.0407	0.0738	0.0523	0.0533
R^2	0.9771	0.8112	0.9840	0.9412	0.9281	0.9438	0.9935	0.9691	0.9298	0.9103
II order										
q_e	8.391	12.874	16.042	18.542	32.191	2.067	4.753	10.497	15.361	24.191
k2	0.0248	0.0151	0.0075	0.0053	0.0041	0.0299	0.0128	0.0087	0.0053	0.0041
R^2	0.9813	0.9984	0.9864	0.9656	0.9415	0.9900	0.9946	0.9724	0.9769	0.9545
Weber Morris										
I	0.1629	−0.0231	−0.0304	0.0357	0.0732	0.1575	−0.1066	0.0400	0.0357	0.0732
K_{id}	0.2329	0.2816	0.6031	0.7997	0.9772	0.1997	0.2628	0.5484	0.7997	0.9772
R^2	0.9027	0.9415	0.9447	0.9147	0.8945	0.9351	0.9873	0.9379	0.9052	0.8829
	Mn(II) Concentration (mg/dm^3)									
	50	100	150	200	250	50	100	150	200	250
I order										
q_e	4.562	7.915	10.596	5.732	5.799	0.345	1.247	1.134	1.186	1.336
k1	0.0688	0.0570	0.1082	0.0899	0.0619	0.0380	0.0332	0.0598	0.1073	0.0845
R^2	0.9767	0.9948	0.9777	0.9606	0.8954	0.9798	0.9604	0.9885	0.8966	0.9915
II order										
q_e	6.534	8.931	10.006	15.472	18.076	1.399	2.369	7.583	12.651	13.729
k2	0.0166	0.0033	0.0071	0.0232	0.0104	0.2777	0.0424	0.0940	0.1657	0.1116
R^2	0.9987	0.9963	0.9874	0.9972	0.9878	0.9984	0.9796	0.9988	0.9987	0.9996
Weber Morris										
I	1.4563	−0.4055	0.9729	4.2850	1.4651	0.9577	0.6015	1.3314	1.8322	1.5328
K_{id}	0.5854	1.0580	0.9987	0.6417	0.7115	0.0515	0.1902	0.1501	0.0998	0.1490
R^2	0.9009	0.9492	0.8300	0.8270	0.9180	0.9361	0.9544	0.9481	0.8665	0.9012
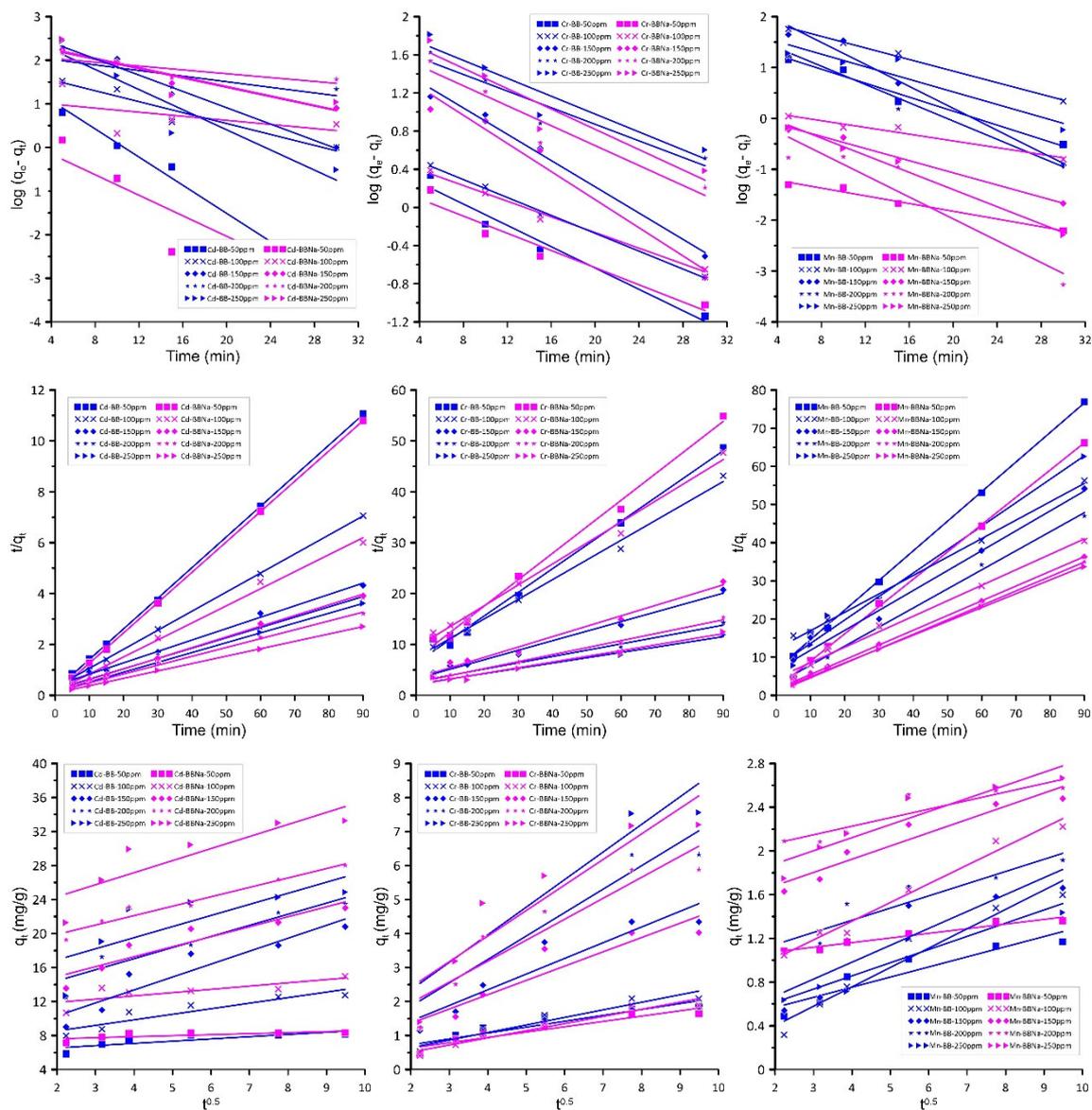
Figure 6. Pseudo–first-rate order, pseudo–second-rate order, and W–M intraparticle diffusion order models for Cd(II), Cr(VI), Mn(II) (50–250 mg/L) and BB and BBNa, respectively.

Carboxyl groups (COOH) play a role in metal ion binding, contributing to the binding capacity of metal ions in biomass through carboxylate ligands. Major constituents of biomass, such as cellulose, pectin, hemicellulose, and lignin, exhibit limited metal ion binding due to the presence of methyl esters [18,29]. However, these methyl esters can undergo modification to form carboxylate ligands upon treatment with a base like sodium hydroxide. This process enhances the biomass's ability to bind metal ions. The hydrolysis reaction of methyl esters is represented as:

$$R\text{-}COOCH_3 + NaOH \rightarrow R\text{-}COO^- + CH_3OH + Na^+$$
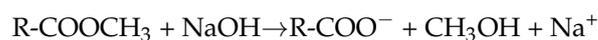
Consequently, chemical modification of biomass increases the abundance of carboxylate ligands, thereby enhancing its metal binding capability, particularly in the context of bioprocessing Mn(II) and Cd(II) ions [30].

3.3. Desorption Studies

One of the primary factors determining the usefulness of sorbent is its potential for reuse. In this study, we investigated the adsorption/desorption properties using different eluents, including 0.1 M organic acids, mineral salts, and water as a control, across five cycles. The obtained results are summarized in Table 6. Studying the values, it can be inferred that the chosen eluents strongly influence desorption. Both BB and BBNa exhibited a decreasing trend in sorption capacity with each successive cycle under optimal adsorption conditions, as depicted in Figure 7. Additional cycles led to a drastic reduction in the sorption capacity of the materials, although this is not presented in the figure.

Table 6. Reusability results of the sorbent in sorption/desorption cycles.

	Elution (%)													
	Cycle 1			Cycle 2			Cycle 3			Cycle 4			Cycle 5		
	Cd(II)	Cr(VI)	Mn(II)	Cd(II)	Cr(VI)	Mn(II)	Cd(II)	Cr(VI)	Mn(II)	Cd(II)	Cr(VI)	Mn(II)	Cd(II)	Cr(VI)	Mn(II)
BB															
Citric acid	84	71	68	80	67	65	78	69	67	80	64	63	74	60	58
Acetic acid	67	59	60	69	55	57	63	52	50	67	50	51	64	48	45
Sodium chloride	19	15	17	20	14	19	22	18	16	15	13	11	11	8	10
Water	0.3	0.1	0.3	0.2	0.1	0.3	0.4	0.2	0.1	0.2	0.5	0.3	0.1	0.2	0.5
BBNa															
Citric acid	80	73	71	78	63	60	75	66	63	74	68	60	69	52	53
Acetic acid	65	61	58	66	50	49	58	46	42	51	43	42	55	40	38
Sodium chloride	21	17	15	18	16	15	11	15	13	12	10	14	15	11	9
Water	0.4	0.1	0.2	0.3	0.1	0.1	0.2	0.3	0.3	0.2	0.4	0.1	0.4	0.3	0.3
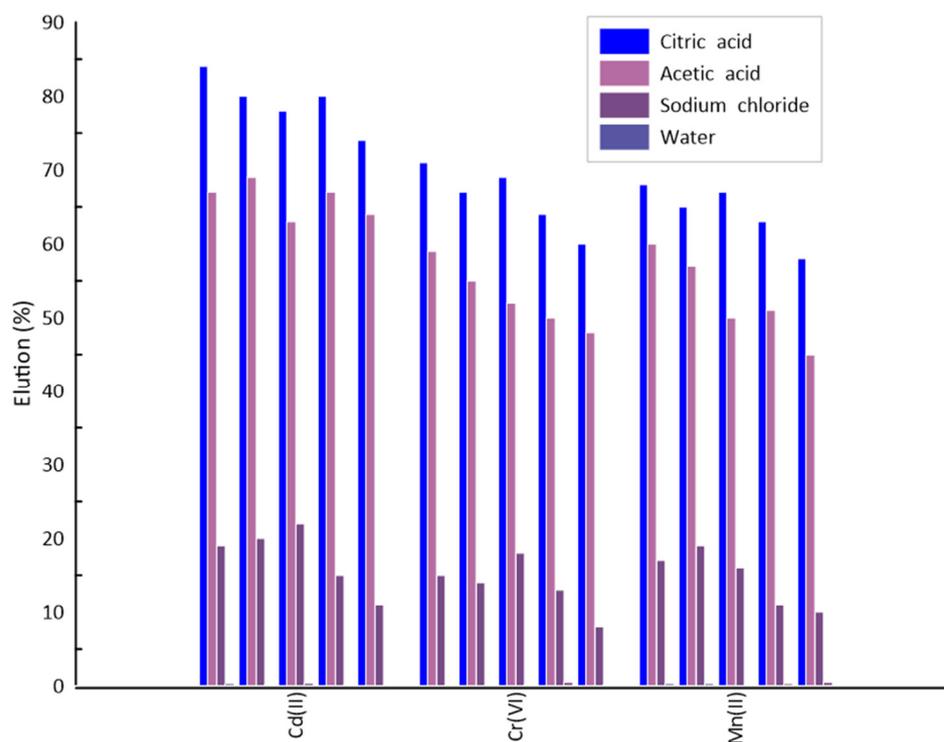
Figure 7. Desorption efficiency of Cd(II), Cr(VI), and Mn(II) after five regeneration cycles.

4. Conclusions

The ability of both unmodified birch bark (BB) and its NaOH-modified version (BBNa) to act as biosorbents for the removal of cadmium, chromium, and manganese ions from aqueous solutions was examined. The modification process demonstrated an enhancement in the bioremediation properties of the material, particularly for cadmium (Cd(II)—33.13 mg/g) and manganese ions (Mn(II)—24 mg/g), attributed to changes in surface charge. Conversely, due to the anionic character of chromates present in water, the raw material exhibited a higher sorption capacity, approximately 36 mg/g for Cr(VI).

SEM–EDS analyses confirmed the adsorption of metal ions onto the materials. Adsorption isotherms and kinetics revealed differences in the processes for cations and anions. According to the best-fitted Langmuir model, manganese(II) ions were adsorbed as a monolayer. Chromium(VI) and cadmium(II) ions' adsorption was best described by the Freundlich isotherm model, suggesting a multilayer ion-adsorbent system with chemisorption dominance, as indicated by $1/n$ values.

The kinetics study for all used sorbents and adsorbents concluded that the process is characterized by the chemical nature of ion binding onto the material surface, aligning with the best fit of the pseudo–second-rate order kinetic model.

References

1. Kulshreshtha, A.; Agrawal, R.; Barar, M.; Saxena, S. A Review on Bioremediation of Heavy Metals in Contaminated Water. *IOSR J. Environ. Sci.* **2014**, *8*, 44–50. [CrossRef]
2. AlOmar, M.K.; Alsaadi, M.A.; Hayyan, M.; Akib, S.; Ibrahim, R.K.; Hashim, M.A. Lead removal from water by choline chloride based deep eutectic solvents functionalized carbon nanotubes. *J. Mol. Liq.* **2016**, *222*, 883–894. [CrossRef]
3. Mani, D.; Kumar, C. Biotechnological advances in bioremediation of heavy metals contaminated ecosystems: An overview with special reference to phytoremediation. *Int. J. Environ. Sci. Technol.* **2014**, *11*, 843–872. [CrossRef]
4. Nzediegwu, C.; Arshad, M.; Ulah, A.; Naeth, M.A.; Chang, S.X. Fuel, thermal and surface properties of microwave-pyrolyzed biochars depend on feedstock type and pyrolysis temperature. *Bioresour. Technol.* **2021**, *320*, 124282. [CrossRef] [PubMed]
5. Bilba, K.; Arsene, M.A.; Ouensanga, A. Study of banana and coconut fibers. Botanical composition, thermal degradation and textural observations. *Bioresour. Technol.* **2007**, *98*, 58–68. [CrossRef]
6. Saleh, I.A.; Zouari, N.; Al-Ghouti, M.A. Removal of pesticides from water and wastewater: Chemical, physical and biological treatment approaches. *Environ. Technol. Innov.* **2020**, *19*, 101026. [CrossRef]
7. Song, H.-J.; Kim, S.; Cho, Y. Removal of heavy metals using sorbents derived from bark. *J. Porous Mater.* **2020**, *27*, 319–328. [CrossRef]
8. Saidi, S.; Boudrahem, F.; Yahiaoui, I.; Aissani-Benissad, F. Agar-agar impregnated on porous activated carbon as a new adsorbent for Pb(II) removal. *Water Sci. Technol.* **2019**, *79*, 1316–1326. [CrossRef]
9. Ighnih, H.; Haounati, R.; Ouachtak, H.; Regti, A.; El Ibrahimi, B.; Hafid, N.; Jada, A.; Taha, M.L.; Addi, A.A. Efficient removal of hazardous dye from aqueous solutions using magnetic kaolinite nanocomposite: Experimental and Monte Carlo simulation studies. *Inorg. Chem. Commun.* **2023**, *153*, 110886. [CrossRef]
10. Das, N.; Vimala, R.; Karthika, P. Biosorption of heavy metals—An overview. *Indian J. Biotechnol.* **2008**, *7*, 159–169.
11. Ding, Z.; Hu, X.; Wan, Y.; Wang, S.; Gao, B. Removal of lead; copper; cadmium; zinc, and nickel from aqueous solutions by alkali-modified biochar: Batch and column tests. *J. Ind. Eng. Chem.* **2016**, *33*, 239–245. [CrossRef]
12. Park, D.; Yun, Y.-S.; Park, J.M.; Past, T. Present, and Future Trends of Biosorption. *Biotechnol. Bioprocess Eng.* **2010**, *15*, 86–102. [CrossRef]
13. Gnanasambandam, R.; Proctor, A. Determination of Pectin Degree of Esterification by Diffuse Reflectance Fourier Transform Infrared Spectroscopy. (n.d.). Available online: https://www.sciencedirect.com/science/article/abs/pii/S0308814699001910 (accessed on 1 December 2023).
14. Pirbazari, A.E.; Saberikhah, E.; Badrouh, M.; Emami, M.S. Alkali treated Foumanat tea waste as an efficient adsorbent for methylene blue adsorption from aqueous solution. *Water Resour. Ind.* **2014**, *6*, 64–80. [CrossRef]
15. Worzakowska, M.; Sztanke, M.; Sztanke, K. Thermal properties and decomposition mechanism of disubstituted fused 1,2,4-triazoles considered as potential anticancer and antibacterial agents. *J. Therm. Anal. Calorim.* **2022**, *147*, 14315–14327. [CrossRef]
16. El Amri, A.; Kadiri, L.; Hsissou, R.; Lebkiri, A.; Wardighi, Z.; Rifi, E.H.; Lebkiri, A. Investigation of Typha Latifolia (TL) as potential biosorbent for removal of the methyl orange anionic dye in the aqueous solution. Kinetic and DFT approaches. *J. Mol. Struct.* **2023**, *1272*, 134098. [CrossRef]
17. Rao, H.; Yang, Y.; Hu, X.; Yu, J.; Jiang, H. Identification of an Ancient Birch Bark Quiver from a Tang Dynasty (A.D. 618-907) Tomb in Xinjiang, Northwest China. *Econ. Bot.* **2017**, *71*, 32–44. [CrossRef]

18. Sidi-Yacoub, B.; Oudghiri, F.; Belkadi, M.; Rodríguez-Barroso, R. Characterization of lignocellulosic components in exhausted sugar beet pulp waste by TG/FTIR analysis. *J. Therm. Anal. Calorim.* **2019**, *138*, 1801–1809. [CrossRef]
19. Gupta, V.K.; Rastogi, A.; Nayak, A. Adsorption studies on the removal of hexavalent chromium from aqueous solution using a low cost fertilizer industry waste material. *J. Colloid Interface Sci.* **2010**, *342*, 135–141. [CrossRef]
20. Khajavian, M.; Wood, D.A.; Hallajsani, A.; Majidian, N. Simultaneous biosorption of nickel and cadmium by the brown algae Cystoseria indica characterized by isotherm and kinetic models. *Appl. Biol. Chem.* **2019**, *62*, 1–12. [CrossRef]
21. Aguilar, D.L.G.; Miranda, J.P.R.; Guzmán, D.B.; Andrés, J.; Muñoz, E.; Co, J.A.E.M. Using Coffee Pulp as Bioadsorbent for the Removal of Manganese (Mn (II)) from Synthetic Wastewater. *Water* **2020**, *12*, 2500. [CrossRef]
22. Sahmoune, M.N. Performance of Streptomyces rimosus biomass in biosorption of heavy metals from aqueous solutions. *Microchem. J.* **2018**, *141*, 87–95. [CrossRef]
23. Svilović, S.; Rušić, D.; Bašić, A. Investigations of different kinetic models of copper ions sorption on zeolite 13X. *Desalination* **2010**, *259*, 71–75. [CrossRef]
24. Kołodyńska, D.; Wnetrzak, R.; Leahy, J.J.; Hayes, M.H.B.; Kwapiński, W.; Hubicki, Z. Kinetic and adsorptive characterization of biochar in metal ions removal. *Chem. Eng. J.* **2012**, *197*, 295–305. [CrossRef]
25. Yang, Y.; Lin, X.; Wei, B.; Zhao, Y.; Wang, J. Evaluation of adsorption potential of bamboo biochar for metal-complex dye: Equilibrium, kinetics and artificial neural network modeling. *Int. J. Environ. Sci. Technol.* **2014**, *11*, 1093–1100. [CrossRef]
26. AL-Othman, Z.A.; Ali, R.; Naushad, M. Hexavalent chromium removal from aqueous medium by activated carbon prepared from peanut shell: Adsorption kinetics, equilibrium and thermodynamic studies. *Chem. Eng. J.* **2012**, *184*, 238–247. [CrossRef]
27. Pacini, V.A.; Ingallinella, A.M.; Sanguinetti, G. Removal of iron and manganese using biological roughing up flow filtration technology. *Water Res.* **2005**, *39*, 4463–4475. [CrossRef] [PubMed]
28. Delgado, N.; Capparelli, A.; Navarro, A.; Marino, D. Pharmaceutical emerging pollutants removal from water using powdered activated carbon: Study of kinetics and adsorption equilibrium. *J. Environ. Manag.* **2019**, *236*, 301–308. [CrossRef]
29. Kaushik, A.; Singh, M. Isolation and characterization of cellulose nanofibrils from wheat straw using steam explosion coupled with high shear homogenization. *Carbohydr. Res.* **2011**, *346*, 76–85. [CrossRef]
30. Bhatti, H.N.; Safa, Y.; Yakout, S.M.; Shair, O.H.; Iqbal, M.; Nazir, A. Efficient removal of dyes using carboxymethyl cellulose/alginate/polyvinyl alcohol/rice husk composite: Adsorption/desorption, kinetics and recycling studies. *Int. J. Biol. Macromol.* **2020**, *150*, 861–870. [CrossRef]